PLANT SCIENCE TODAY
ISSN 2348-1900 (online)
Vol x(x): xx–xx
https://doi.org/10.14719/pst.4576

HORIZON
e-Publishing Group
HePG

RESEARCH ARTICLE

Estimation of actual evapotranspiration using surface energy balance algorithm for land in the lower Bhavani basin

Pavithran P[1], Pazhanivelan S[2]*, Sivamurugan AP[2], Ragunath KP[2], Selvakumar S[2], Vanitha K[3] & Kannan P[2]

[1]Department of Agronomy, Tamil Nadu Agricultural University, Coimbatore, Tamil Nadu -641003, India

[2]Centre for Water and Geospatial Studies, Tamil Nadu Agricultural University, Coimbatore, Tamil Nadu -641003, India

[3]Department of Fruit Science, Tamil Nadu Agricultural University, Coimbatore, Tamil Nadu -641003, India

*Email: pazhanivelans@tnau.ac.in

OPEN ACCESS

ARTICLE HISTORY

Received: 07 August 2024
Accepted: 10 September 2024

Available online
Version 1.0 : 04 October 2024

Check for updates

Additional information

Peer review: Publisher thanks Sectional Editor and the other anonymous reviewers for their contribution to the peer review of this work.

Reprints & permissions information is available at https://horizonepublishing.com/journals/index.php/PST/open_access_policy

Publisher's Note: Horizon e-Publishing Group remains neutral with regard to jurisdictional claims in published maps and institutional affiliations.

Indexing: Plant Science Today, published by Horizon e-Publishing Group, is covered by Scopus, Web of Science, BIOSIS Previews, Clarivate Analytics, NAAS, UGC Care, etc
See https://horizonepublishing.com/journals/index.php/PST/indexing_abstracting

CITE THIS ARTICLE

Pavithran P, Pazhanivelan S, Sivamurugan AP, Ragunath KP, Selvakumar S, Vanitha K, Kannan P. Estimation of Actual Evapotranspiration Using Surface Energy Balance Algorithm for Land in the Lower Bhavani Basin. Plant Science Today (Early Access).
https:/doi.org/10.14719/pst.4576

Abstract

Evapotranspiration is a vital process that substantially sustains the hydrothermal balance. The spatial and temporal assessment of evapotranspiration is critical for the management of water resources and drought monitoring at a regional scale. Surface Energy Balance Algorithm for Land (SEBAL) was employed to compute daily actual evapotranspiration in the lower Bhavani basin using Landsat 8 imagery, weather data and digital elevation model. The study aimed to analyze the spatial and temporal distribution of evapotranspiration. In addition, the influence of surface parameters such as surface albedo, land surface temperature, normalized difference vegetation index and net radiation flux on evapotranspiration was also investigated. The results revealed that SEBAL estimates agreed to 86.5 per cent with pan evaporation. Surface evapotranspiration showed seasonal variability with lower rates during winter and recorded maximum evapotranspiration during summer. Land use classes such as flooded vegetation and water bodies were found to have higher rates of mean daily evapotranspiration, whereas bare soil had lower evapotranspiration. Net radiation was noticed to have a significant impact on daily evapotranspiration among surface parameters. Hence, SEBAL can produce accurate evapotranspiration estimates for the study area. Moreover, vegetation cover and hydrothermal conditions significantly affect the surface parameters, which considerably affect surface evapotranspiration.

Keywords

Evapotranspiration; land cover; SEBAL; surface parameters

Introduction

Evapotranspiration is a crucial component of the hydrological cycle, encompassing soil surface evaporation and vegetation transpiration (1, 2). It is a continuous energy flux among the hydrosphere, atmosphere and biosphere (3, 4). Evapotranspiration substantially affects the redistribution of water from the Earth's surface back into the atmosphere, thereby influencing regional and global water balance. It has been noticed that sixty percent of the precipitation is lost to the atmosphere through the evapotranspiration process; however, it was found to be higher in arid regions (5). Moreover, evapotranspiration (ET) acts as a mechanism for energy transfer, regulates the Earth's surface temperature and influences climate dynamics. The interaction between evapotranspiration and other water cycle components underscores the significance of evapotranspiration in sustaining water

resources and ecosystem health. Therefore, evapotranspiration is a critical element in the global water cycle and a key parameter for water resource management, hydrological modelling and assessment of climate change (6). Estimating evapotranspiration necessitates efficient use of water resources, ecosystem conservation for sustainable management practices and informed decision-making.

Accurate evapotranspiration estimation methods, including lysimetry, eddy covariance and empirical methods, are employed to study water dynamics under different ecological conditions. However, methods have several limitations, such as being expensive and laborious and providing estimates for specific site of location. It restricts the applicability of such techniques in large-scale monitoring and broader environmental assessments, posing challenges in obtaining comprehensive data over extensive regions. It emphasizes the need for more feasible and cost-effective methods for accurately estimating evapotranspiration across diverse landscapes and larger spatial scales. Spatio-temporal assessment techniques comprehensively analyze evapotranspiration dynamics over larger geographical areas and multiple time scales (7). Remote sensing techniques involve satellites equipped with optical and thermal sensors and advanced modelling approaches to estimate evapotranspiration at regional and global scales (8). It provides valuable insights into evapotranspiration's spatial distribution and temporal variability and facilitates land use planning, water resource management and adaptation strategies to climate change (9).

Moreover, it enables the computation of actual evapotranspiration for a region of interest with limited ground observations. It helps to identify areas vulnerable to water stress and continuously monitor changes in hydrological regimes over time. Various remote sensing-based ET models such as Surface Energy Balance Algorithm for Land (SEBAL), Mapping Evapotranspiration at High Resolution with Internalized Calibration (METRIC), Atmosphere-Land Exchange Inverse (ALEXI), Simplified Surface Energy Balance (SSEB), Surface Energy Balance System (SEBS), etc. are employed to assess the evapotranspiration in the recent years (10-12).

Surface Energy Balance Algorithm for Land is advantageous over other methods due to the wide range of applications, higher accuracy and required limited ground truth collections (13). The model was developed by Bastiaanssen, a physical approach that estimates evapotranspiration as a residual of surface energy balance using remote sensing and local meteorological datasets (14). SEBAL is a commonly accepted model to estimate evapotranspiration across different countries (15). The model was validated for various regions, and accuracy was about 85 per cent (16, 17). For instance, the actual evapotranspiration of corn was assessed by utilizing the SEBAL algorithm and validated ET estimates against the Penman-Monteith method, a classical approach in the estimation of crop evapotranspiration (18). The findings indicated a strong relationship between SEBAL-ET estimates and the Penman-Monteith method with less root mean square error (1.14). Similarly, SEBAL can produce reliable ET estimates, with a correlation coefficient 0.97 compared to the Penman-Monteith method (19).

The Lower Bhavani basin is characterized by diverse ecological conditions and experiences moderate rainfall and intense surface evapotranspiration. Evapotranspiration poses a significant impact on regional climate patterns. Assessment of evapotranspiration is crucial for various applications such as agricultural water management, climatology studies and hydrological assessments. Therefore, the study was carried out to assess the spatio-temporal distribution of actual evapotranspiration using the SEBAL algorithm, validate the accuracy of SEBAL ET with ground data and study the influence of surface parameters on evapotranspiration in the lower Bhavani basin.

Materials and Methods

Study area

The Lower Bhavani basin, area selected for the present study is a part of the Cauvery basin, encompassing major parts of Erode and some parts of Coimbatore and Tiruppur districts (Fig. 1). The study area is situated between latitudes 11° 15′ and 11° 45′ N and longitudes 77° 0′ E and 77° 40′ E, covering a geographical area of 2402 km^2. It comprises diverse landscapes such as forests, water bodies, croplands, barren land and settlements. The basin has varied topography ranging from 154 m to 1669 m. The region experiences a semi-arid climate, with an annual rainfall of 666.84 mm and temperature ranging from 22 to 42 °C. The diversified features significantly impacted the hydrology, agriculture and overall ecosystem dynamics of the basin.

Data Sources

Landsat 8 imagery covering the study area, precisely path 144 and row 52, was acquired from the United States Geological Survey (USGS) Earth Explorer platform. Images were selected with clover cover having less than 10 per cent to obtain reliable evapotranspiration estimates. Similarly, Digital Elevation Model (DEM) data with a spatial resolution of 30 m was downloaded from the Shuttle Radar Topographic Mission (SRTM) database, accessible through USGS Earth Explorer (Fig. 2). The satellite imagery was acquired for the year 2023 to assess the spatio-temporal distribution of evapotranspiration and the influence of surface parameters. Meteorological data provided by the European Centre for Medium-Range Weather Forecasts (ECMWF) Reanalysis v5 (ERA5) dataset was used to obtain evapotranspiration. Sentinel 2 land use land cover with a spatial resolution of 10 m was downloaded from the ESRI platform to assess the evapotranspiration rate of different land use classes (Fig. 3).

Methodology

The Surface Energy Balance Algorithm for Land is a widely used model developed by Bastiaanssen in the 1990s. Subsequently, it was refined and adopted for various applications in agriculture, hydrology and climatology.

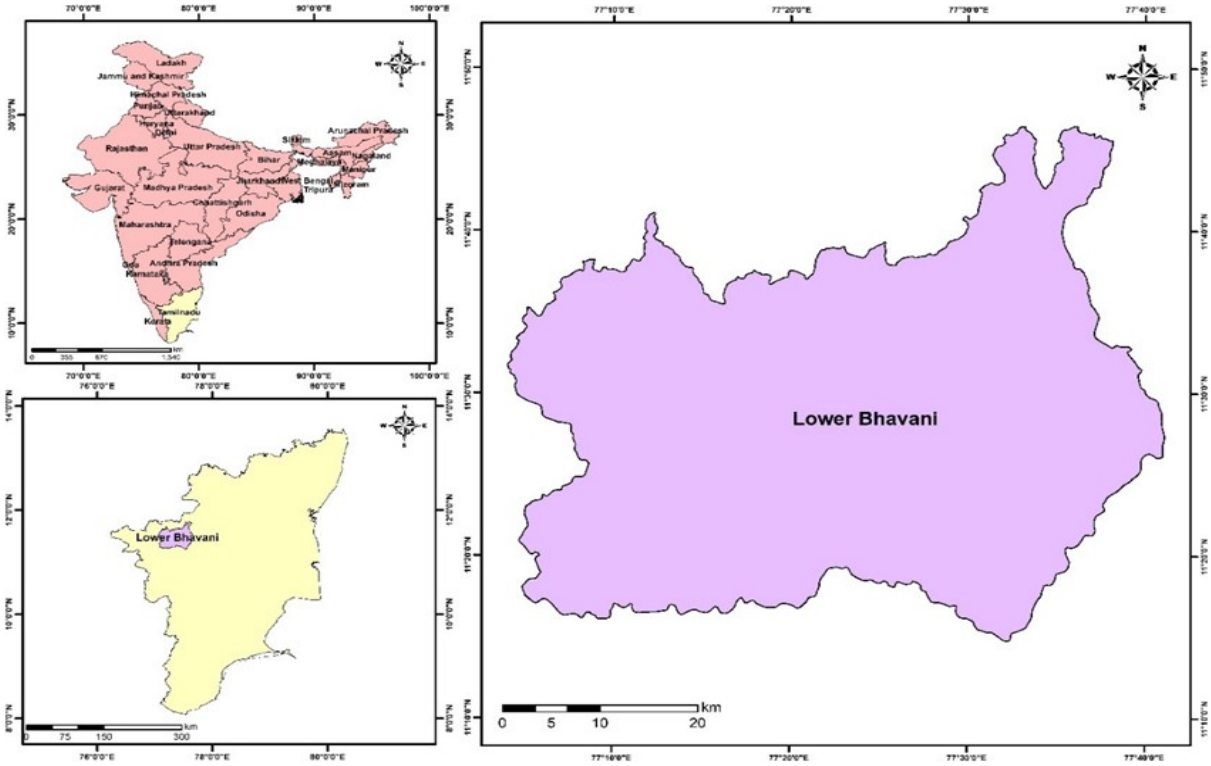

Fig. 1. Map of the study area

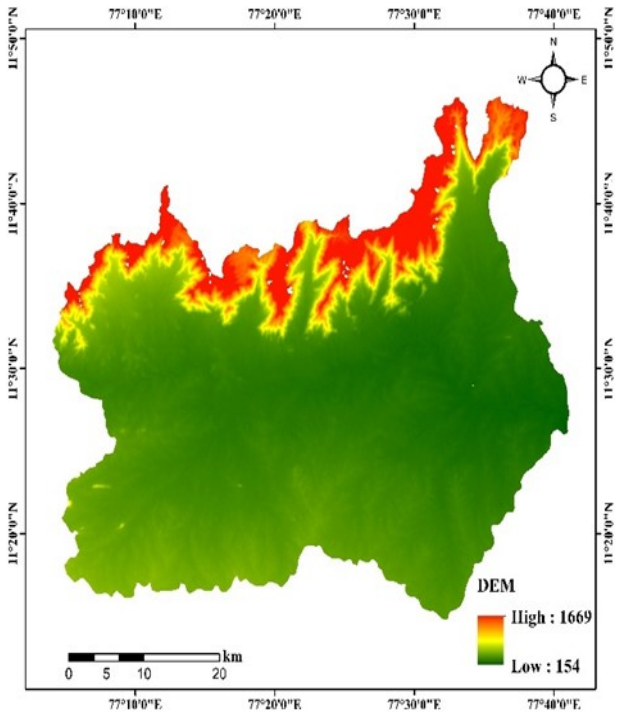

Fig. 2. DEM of the lower Bhavani basin

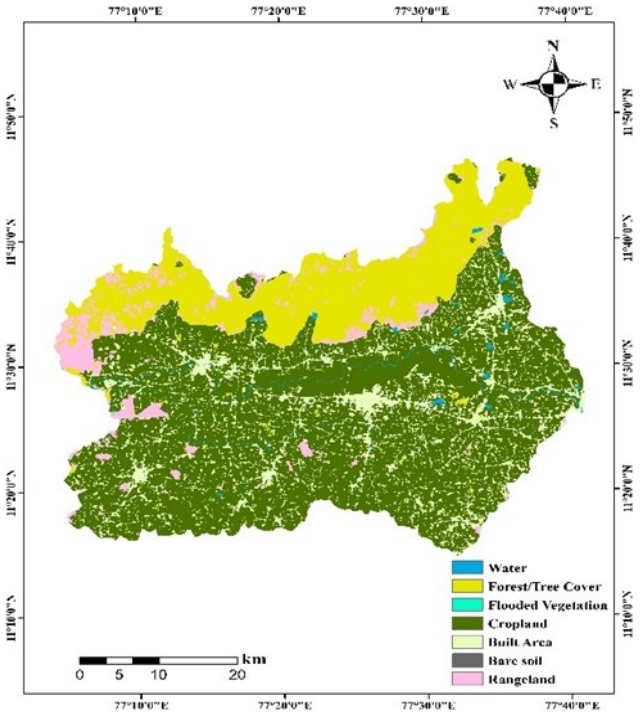

Fig. 3. LULC of the study area

SEBAL model provides evapotranspiration estimates by combining satellite-derived thermal infrared imagery with meteorological data and a digital elevation model. It relies on remote sensing data, advantageous in areas with limited ground observations. SEBAL algorithm is based on the physical principle of energy balance and offers a mechanistic understanding of land-atmosphere interactions, which is suitable for scientific research and hydrological modelling applications. It operates by computing various energy balance components such as net solar radiation, sensible heat flux, soil heat flux and latent heat flux. It calculates the instantaneous ET flux for each image pixel as a residual of surface energy balance (14).

$$\lambda ET = R_n\text{-}G\text{-}H \qquad \textbf{(Eqn.1)}$$

Where λET is the instantaneous latent heat flux (W/m^2), R_n is the net solar radiation (W/m^2), G is the soil heat flux (W/m^2) and H is the sensible heat flux (W/m^2). Google Earth Engine script was used to execute the SEBAL model to obtain daily evapotranspiration for the study area.

Net radiation flux

Net radiation flux is the energy available at the surface and expressed in W/m^2. It is worked out as the difference between incoming and outgoing radiant fluxes. Net surface radiation flux is obtained as follows,

$$R_n = (1-\alpha)R_s\downarrow + RI\downarrow - RI\uparrow - (1-\varepsilon_o)\, RI\downarrow \quad \textbf{(Eqn.2)}$$

$$R_s\downarrow = G_{SC} \times \cos\theta \times d_r \times T_{sw} \quad \textbf{(Eqn.3)}$$

$$d_r = 1+0.033 \cos\left(DOY \times \frac{2\pi}{365}\right) \quad \textbf{(Eqn.4)}$$

$$T_{sw} = 0.75 + 2 \times 10^{-5} \times Z \quad \textbf{(Eqn.5)}$$

$$RI\uparrow = \varepsilon_o \times \sigma \times T^4_s \quad \textbf{(Eqn.6)}$$

$$RI\downarrow = \varepsilon_a \times \sigma \times T^4_a \quad \textbf{(Eqn.7)}$$

$$\varepsilon_a = 0.85 \times (-\ln T_{sw})^{0.09} \quad \textbf{(Eqn.8)}$$

$$\alpha = \frac{\alpha_{toa} - \alpha_{path\_radiance}}{T_{sw}^2} \quad \textbf{(Eqn.9)}$$

where, $R_s\downarrow$ is the shortwave incoming solar energy that reaches the Earth's surface (W/m^2), $RI\downarrow$ is the long wave radiation from the atmosphere to the Earth's surface (W/m^2), $RI\uparrow$ is the thermal radiation emitted from the surface (W/m^2), α is the surface albedo, ε_o is the surface emissivity, G_{sc} is the solar constant (1367 W/m^2), cosθ is the cosine of solar incidence angle, d_r is the inverse squared relative earth-sun distance, T_{sw} is the atmospheric transmissivity, DOY is the days of the image in the current year, Z is the elevation above the sea level, σ is the Stefen Boltzmann constant (5.67x10^{-8} W/m^2 K^4), T_s is the land surface temperature (K), T_a is the near-surface air temperature (K), ε_a is the atmospheric emissivity, α_{toa} is the albedo at the top of the atmosphere and $\alpha_{path\_radiance}$ is the average fraction of solar radiation backscattered before it reaches the Earth's surface.

In addition, normalized difference vegetation index (NDVI) and land surface temperature (LST) were estimated by using the following equations during the computation of net radiation flux,

$$NDVI = \frac{\rho_4 - \rho_3}{\rho_4 + \rho_3} \quad \textbf{(Eqn.10)}$$

$$LST = \frac{K_2}{\ln\left(\frac{\varepsilon_{NB} K_1}{R_C} + 1\right)} \quad \textbf{(Eqn.11)}$$

where, ρ_4 and ρ_3 are reflectivity of near-infrared and red bands, respectively. K_1 and K_2 are constants for thermal bands, respectively. ε_{NB} is the emissivity of narrowband, and R_c is the corrected thermal radiance.

Soil heat flux

Soil heat flux represents the heat storage rate in the soil due to the temperature gradient between surface air and soil. The process of conduction, which results in the transmission of energy, commonly drives it. Soil heat flux contributes substantially to the energy balance, primarily affected by land use cover and topography. It is difficult to derive the soil heat flux directly and Bastiaanssen (20) subsequently proposed the following empirical formula: the ratio of soil heat and net radiation fluxes.

$$G = R_n \times \frac{T_s - 273.15}{\alpha}\left(0.0038\alpha + 0.0074\alpha^2\right)\left(1-0.98 \times NDVI^4\right) \quad \textbf{(Eqn.12)}$$

Sensible heat flux

Sensible heat flux indicates the rate of heat loss to the atmosphere by conduction and convection due to the temperature difference between the air and the Earth's surface. It is mainly determined by surface temperature gradient, roughness and wind speed. It is calculated as follows (21),

$$H = \frac{\rho_{air} \times C_p \times dT}{r_{ah}} \quad \textbf{(Eqn.13)}$$

where, ρ_{air} denotes air density (kg/m^3), C_p is the specific heat of the air (1004 J/kg/K), dT and r_{ah} are two unknown factors represent the temperature difference between two heights (Z_1 and Z_2) and aerodynamic resistance to the heat transport (s/m), respectively. dT is computed using two anchor pixels, *viz.* hot and cold pixels. The cold pixel indicates the pixel of the well-irrigated crop with full vegetation cover and the hot pixel represents bare soil assumed to be zero. Moreover, a linear correlation between dT and LST was considered to obtain the sensible heat flux.

$$r_{ah} = \frac{\ln\left(\frac{Z_2}{Z_1}\right)}{u_* \times k} \quad \textbf{(Eqn. 14)}$$

where λET is

$$u_* = \frac{u_x \times k}{\ln\left(\frac{Z_x}{Z_{0m}}\right)} \quad \textbf{(Eqn. 15)}$$

u_* is the friction velocity (m/s), k is the Von Karman's constant (0.41), u_x is the wind velocity (m/s) at height z_x and z_{om} is the zero-momentum roughness length (m).

$$\lambda ET = R_n - G - H \quad \textbf{(Eqn.16)}$$

Latent heat flux

Latent heat flux is the critical parameter that indicates the energy exchange between the atmosphere and Earth. It is the residual energy balance available for water vaporization from soil and

$$ET_{inst}(mm/h) = \frac{\lambda ET \times 3600}{\lambda} \quad \textbf{(Eqn.17)}$$

plant surfaces. It is computed by calculating for each pixel by the following equation (14, 22),

Subsequently, instantaneous evapotranspiration (ET_{inst}) is obtained as follows,

Where λ represents latent heat of vaporization (J/kg), 3600 is the conversion factor for seconds to hour (h).

Daily evapotranspiration

$$ET_rF = \frac{ET_{inst}}{ET_r} \quad \textbf{(Eqn.18)}$$

The reference evapotranspiration fraction *(ET_rF)* was computed to obtain the daily actual evapotranspiration. It is calculated as the ratio of instantaneous evapotranspiration to the reference ET for each image pixel. Reference *ET (ET_r)* during the satellite pass was derived using REF-ET software with the help of weather variables downloaded from the NASA power platform. It is assumed that computed ET_rF is constant for the day. Later, daily actual evapotranspiration (ET_{24}) is estimated by multiplying ET_rF with daily reference ET(ET_{r24}) (18).

$$ET_{24} = ET_rF \times ET_{r24} \quad \textbf{(Eqn.19)}$$

Spatial and temporal analysis of daily evapotranspiration

Daily evapotranspiration of different dates was assessed and validated with pan evaporation data from the weather station in the study area. Similarly, the spatial distribution of evapotranspiration across different land cover was studied using the sentinel 2 land cover dataset and mean daily evapotranspiration was worked out. Surface parameters such as surface albedo, LST and NDVI are essential inputs in the SEBAL model, which are sensitive to changes in land use, climate and vegetation cover, significantly influencing the daily evapotranspiration. Hence, the influence of surface parameters on evapotranspiration was assessed to understand the impact within the study area. Moreover, the effect of different energy fluxes on daily evapotranspiration was also studied. The correlation study was carried out using ArcGIS 10.8 and R 4.4.1 software.

Results and Discussion

The estimation of daily actual evapotranspiration relies on the assumption that the reference evapotranspiration fraction accurately represents the prevailing conditions of the day. The zonal statistics tool in ArcGIS software was used to obtain the daily mean evapotranspiration for each satellite pass and different land use cover. The spatio-temporal distribution of evapotranspiration in the study area was primarily influenced by hydrothermal conditions (23), resulting in significant variations in evapotranspiration rates over different periods (Table 1). The lower amount of evapotranspiration was noticed during January, mainly attributed to limited hydrothermal conditions during winter. Lower temperature and precipitation generally reduce the capacity of water to evaporate from the soil surface and transpire from vegetation. Subsequently, it increased consistently and achieved maximum during summer in April. The higher daily evapotranspiration rate was due to increased air temperature and the beginning of crop season (Fig. 4).

Table 1. Daily average evapotranspiration in the lower Bhavani basin

S.No.	Date	Mean ET (mm/day)	Standard Deviation
1.	03.01.2023	3.54	0.77
2.	19.01.2023	4.59	1.16
3.	20.02.2023	4.76	1.28
4.	08.03.2023	5.52	1.90
5.	09.04.2023	5.88	1.96
6.	27.05.2023	5.54	1.29
7.	15.08.2023	5.58	1.61

The surface evapotranspiration estimated using the SEBAL algorithm is crucial to validate for various applications. The accuracy assessment was conducted with open pan evaporation data from the local meteorological weather station. The agreement (d) between SEBAL estimates and pan evaporation was 86.5 per cent with root mean square error (RMSE) and normalized root mean square error (NRMSE) of 0.69 and 13.49, respectively (Fig. 5). The agreement results demonstrated that SEBAL algorithm could be employed to assess the daily actual evapotranspiration with greater accuracy in the lower Bhavani basin. The results were consistent with the findings of previous studies (24, 25), and SEBAL estimates were comparable with pan evaporation. Further, using remote sensing data, SEBAL provides spatial evapotranspiration estimates with greater accuracy across large areas. It enables detailed evapotranspiration mapping across different land covers, which is crucial for sustainable water management. SEBAL have greater significance for estimating evapotranspiration over various time scales, allowing for continuous monitoring and temporal analysis. At the same time, conventional methods depend on periodic measurements, resulting in less accurate evapotranspiration estimates.

Moreover, the spatial distribution of evapotranspiration over different land use classes was studied. The findings indicated that the amount of moisture lost in evapotranspiration immensely varied with different land use classes (Table 2). Forests were observed to have higher evapotranspiration, followed by water bodies. The vegetation factors, such as type and density, significantly impact evapotranspiration. Dense forest cover with tall trees and water drains in the study area caused elevated evapotranspiration compared to other land use classes. The consistent water supply during

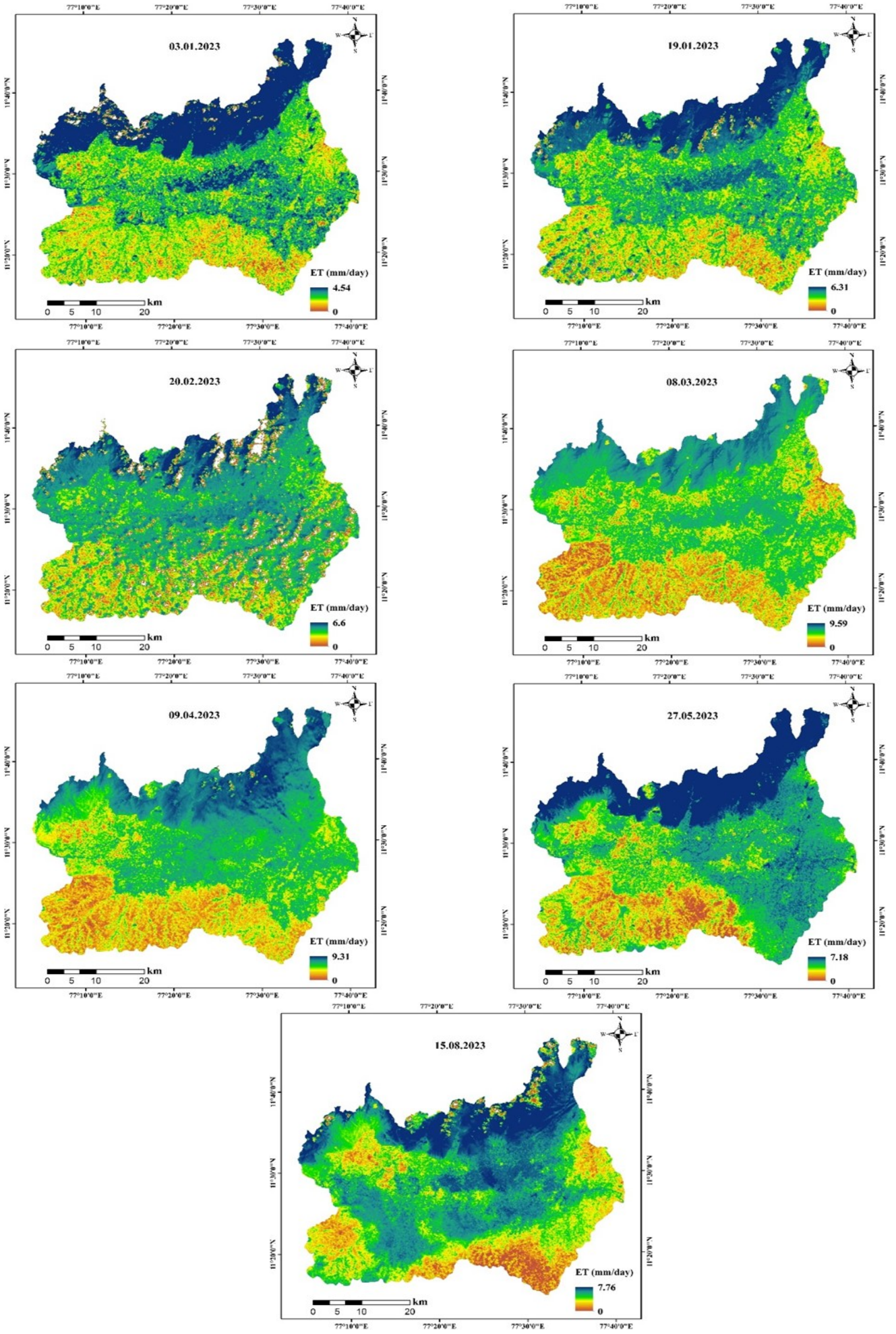

Fig. 4. Spatio-temporal distribution of evapotranspiration in the lower Bhavani basin

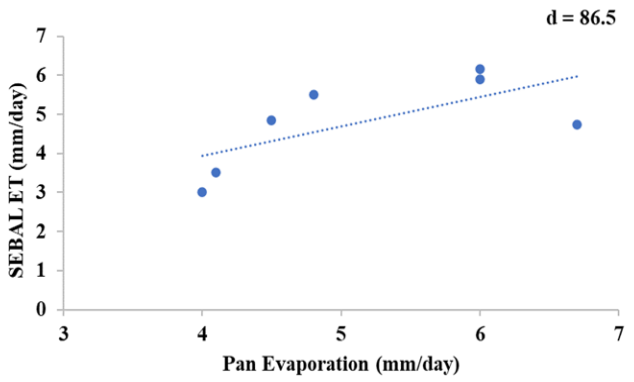

Fig. 5. Comparison of pan evaporation and SEBAL ET

Table 2. Mean daily evapotranspiration for various land use classes

S.No.	Land use class	Mean daily ET (mm/day)
1.	Cropland	4.67
2.	Forest	6.64
3.	Waterbody	6.41
4.	Rangeland	5.48
5.	Settlement	4.50
6.	Barrenland	4.28
7.	Flooded vegetation	6.23

evaporation and reduced boundary layer resistance in the water body favoured more water loss. Cropland was recorded with average evapotranspiration of 4.67 mm/day and was primarily influenced by soil moisture availability and management practices. The major crops in the study area are rice, banana and sugarcane, mainly cultivated under irrigated conditions and provide moisture for evapotranspiration loss. Barrenland recorded lower values of evapotranspiration followed by settlement due to limited soil moisture. The settlement comprised build-up land with vegetation that was attributed to more evapotranspiration. A similar trend of evapotranspiration rates was reported across different land use types (24, 26, 27). The study employed Landsat 8 datasets, providing evapotranspiration estimation with a high spatial resolution of 30 m. It is crucial for areas with diverse landscapes where higher spatial resolution provides accurate evapotranspiration dynamics across various land cover. However, the temporal resolution of the dataset utilized was 16 days, which limits the ability to monitor the rapid temporal changes in evapotranspiration, particularly during dynamic agricultural growth periods or in regions with frequent cloud cover. It can be addressed by employing data fusion techniques and advanced cloud-gap filling algorithms, which would enhance the continuity and accuracy of evapotranspiration estimates using the SEBAL algorithm, resulting in more reliable and significant estimates.

Surface parameters significantly influence energy transmission and surface evapotranspiration (Fig. 6-10). Surface parameters are closely related to land use and land cover, which substantially affect evapotranspiration. Surface albedo indicates the proportion of total incident radiation reflected by the Earth. It is a critical parameter that determines the partitioning of net radiation into soil heat and sensible heat fluxes. Surfaces with lower albedo absorb more incident solar radiation and increasing surface temperature results in a higher evapotranspiration rate.

Conversely, snow, ice and bare soil have a high albedo effect, reducing evapotranspiration. Surface albedo is generally dynamic and influenced by various factors, including solar elevation angle, soil surface, soil moisture, soil texture, vegetation cover, etc. (28, 29). The correlation analysis demonstrated that surface albedo has an inverse effect on evapotranspiration. Similarly, land surface temperature was also significantly influenced by the evapotranspiration process and mainly determined by water vapour and surface emissivity. A negative correlation was observed between land surface temperature and daily evapotranspiration. It is common in regions with diversified landscapes and results are consistent with the interpretation of previous studies (30).

For instance, areas with homogenous weather variables such as air temperature, humidity, wind speed and solar radiation have a higher evapotranspiration rate with lower surface temperature (31). The spatio-temporal variation between land surface temperature and evapotranspiration primarily caused by vegetation cover, soil moisture availability and surface roughness. In addition, results revealed that NDVI exhibited a positive approach to daily evapotranspiration. Vegetation with higher NDVI values is strongly associated with adequate soil moisture availability and dense vegetation cover, which is attributed to more transpiration (32).

Moreover, net radiation indicates the balance between incoming and outgoing solar radiation at the Earth's surface. The spatial distribution of net radiation poses a significant effect and determines the energy available to drive the evapotranspiration process. Higher evapotranspiration was noticed with an increased amount of net radiation. The results revealed that net radiation exhibited a higher relationship with daily evapotranspiration, followed by NDVI, surface temperature and surface albedo. The results on the effect of surface parameters on daily evapotranspiration were corroborated with the previous findings (24, 27, 33, 34). Conventional evapotranspiration estimation methods depend on average conditions or simplified models that may not adequately account for the local variations in surface characteristics, resulting in less accurate estimates. Conversely, SEBAL offers significant advantages by directly incorporating the land surface heterogeneity, including vegetation cover, surface temperature, surface albedo, etc., into estimating actual evapotranspiration. It is particularly critical in regions with diverse land covers, where an accurate representation of spatial variability is required.

Water bodies and flooded vegetation recorded lower albedo effects and absorbed higher net radiation levels, resulting in higher evapotranspiration among land use classes. The northern part of the study area comprises dense forest, which was observed with lower albedo and higher NDVI over different periods, causing higher

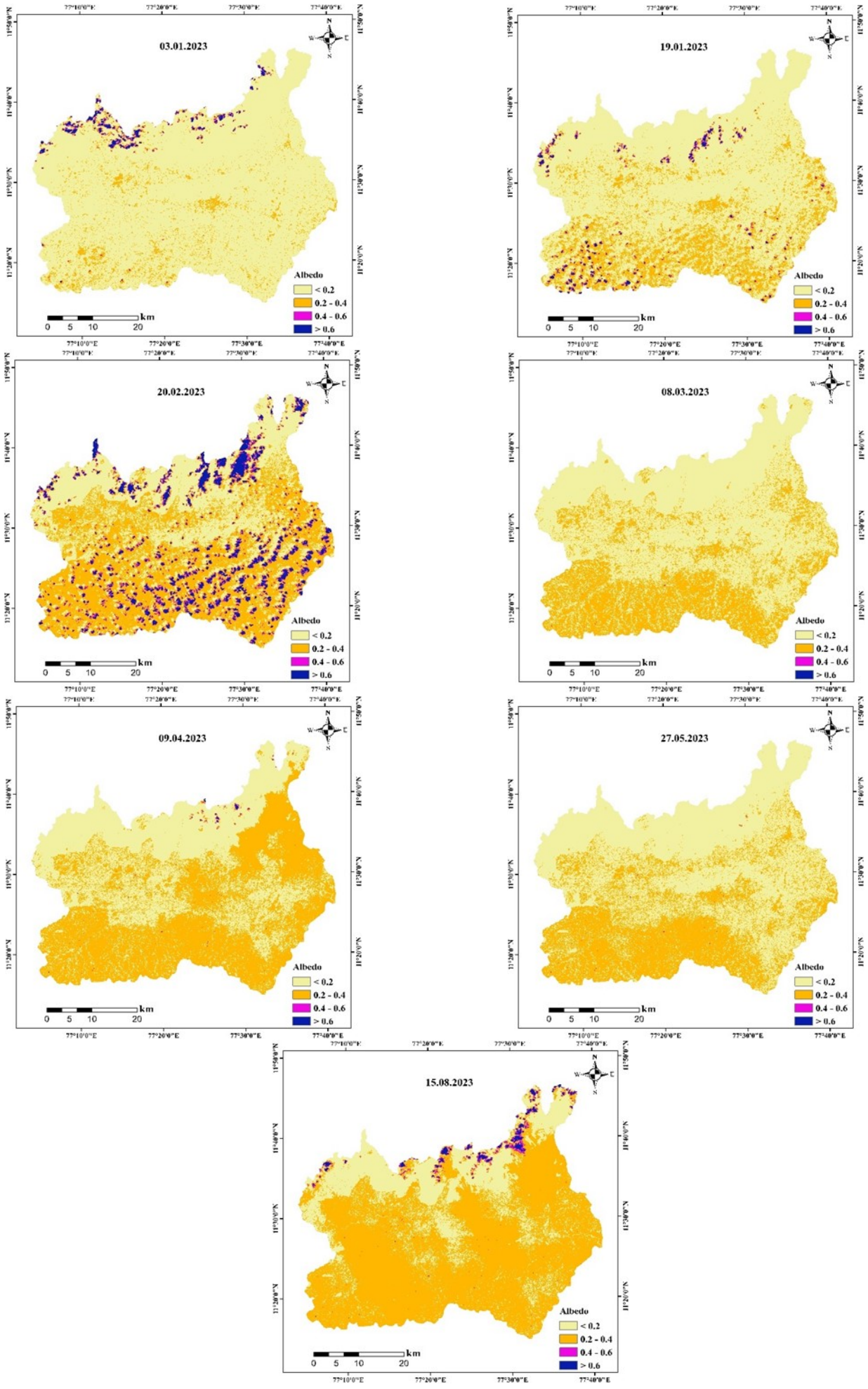

Fig. 6. Spatio-temporal variation of surface albedo

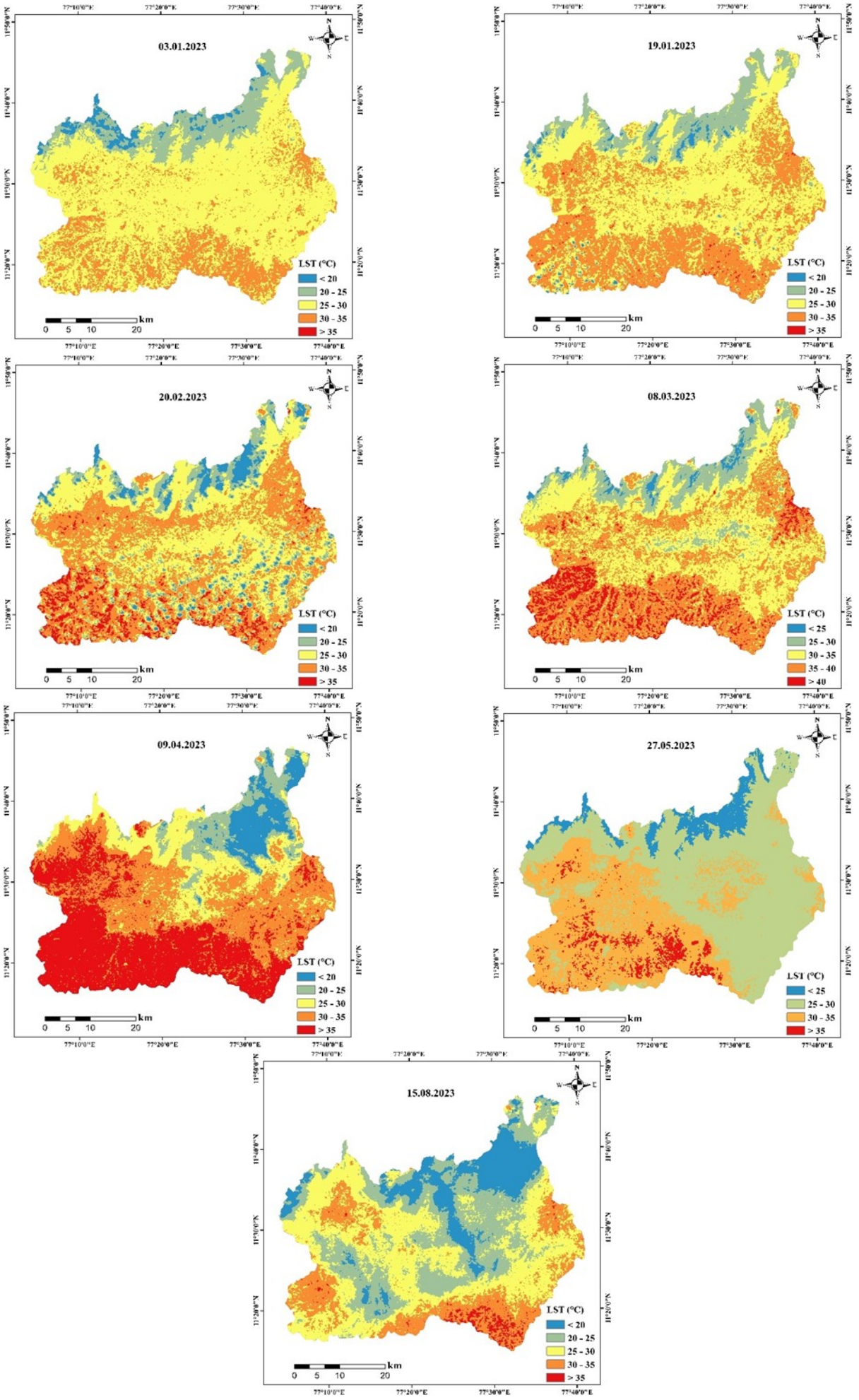

Fig. 7. Spatio-temporal distribution of LST

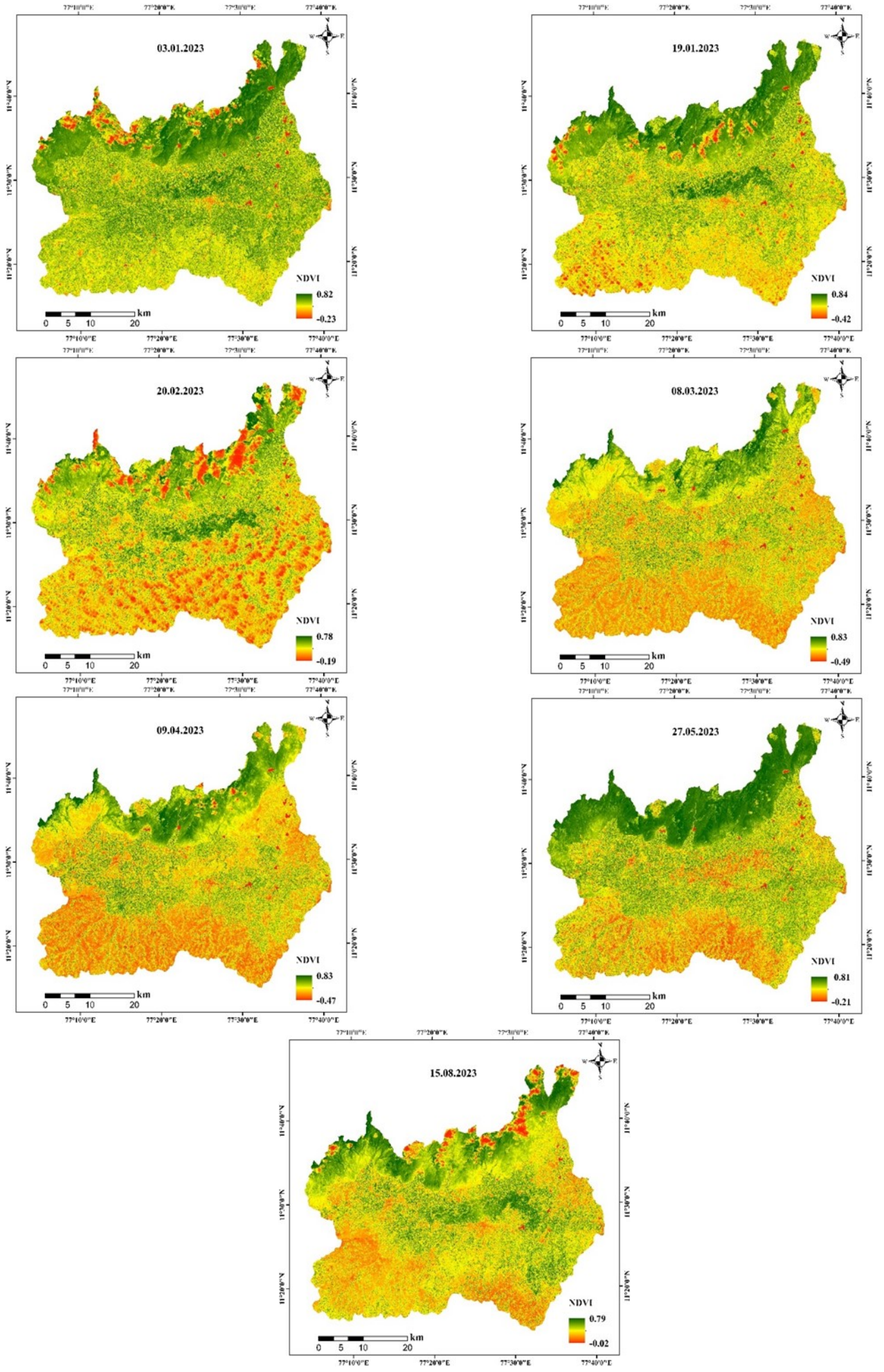

Fig. 8. Spatio-temporal variation of NDVI

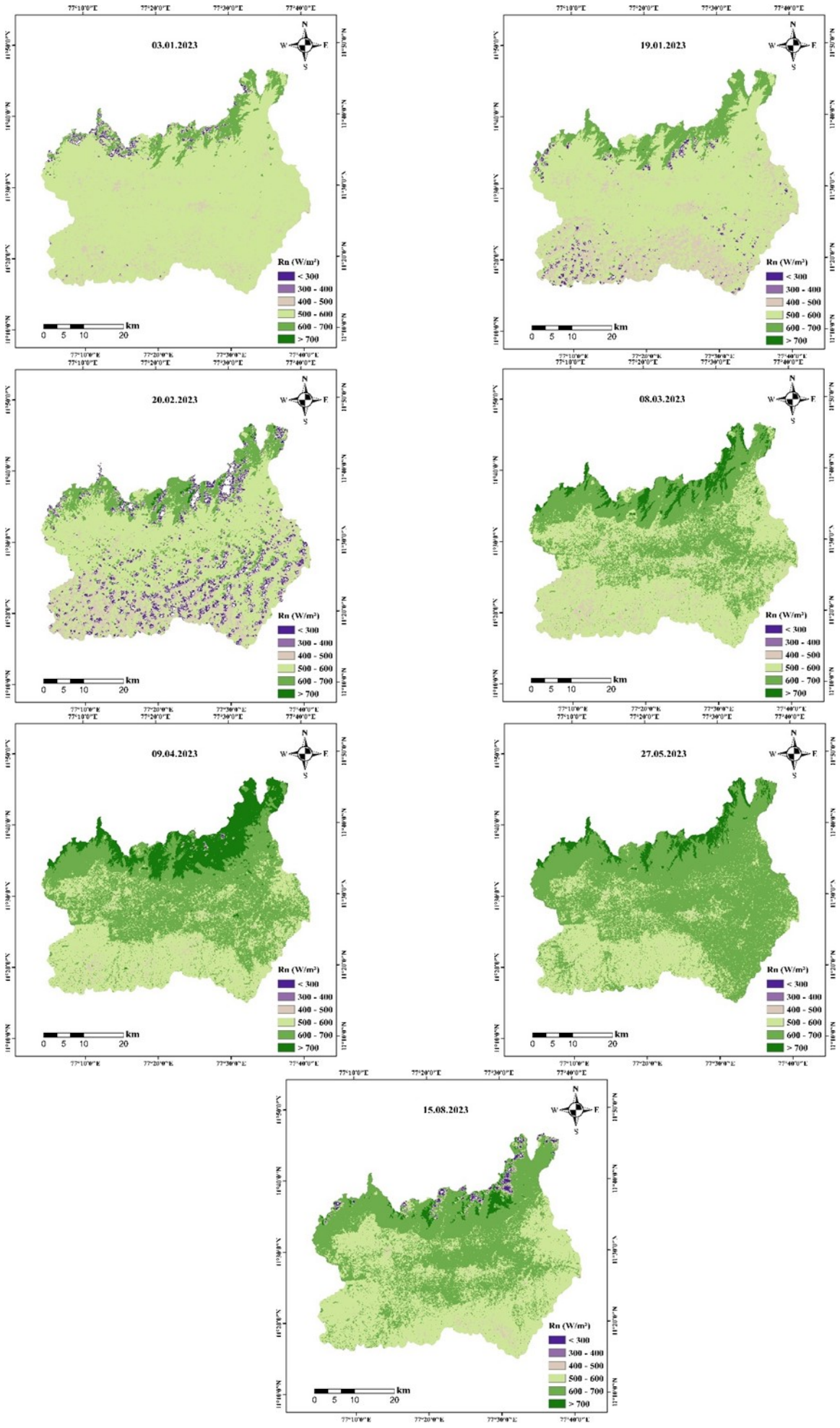

Fig. 9. Spatio-temporal distribution of net radiation

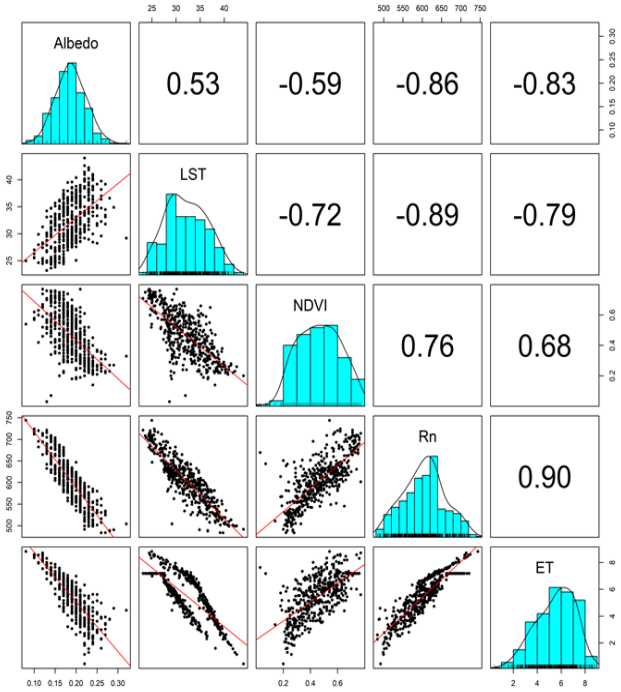

Fig. 10. Correlation among surface variables and daily evapotranspiration

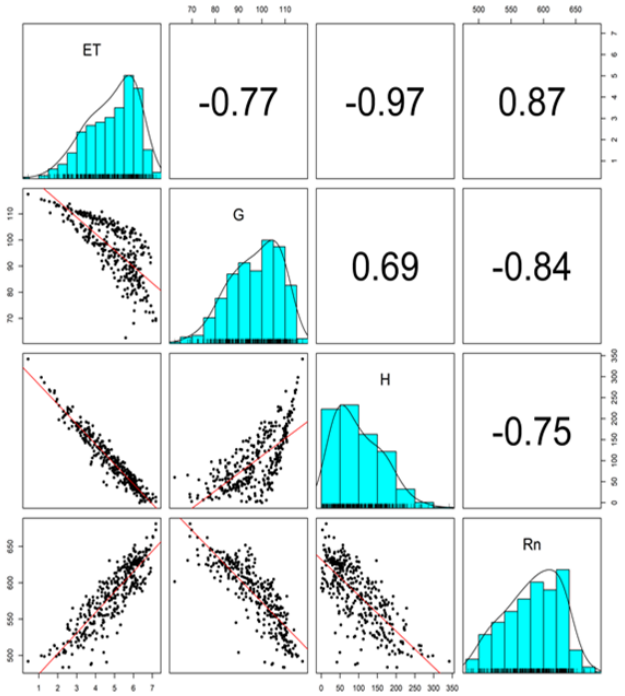

Fig. 12. Relationship between different surface energy balance components and evapotranspiration

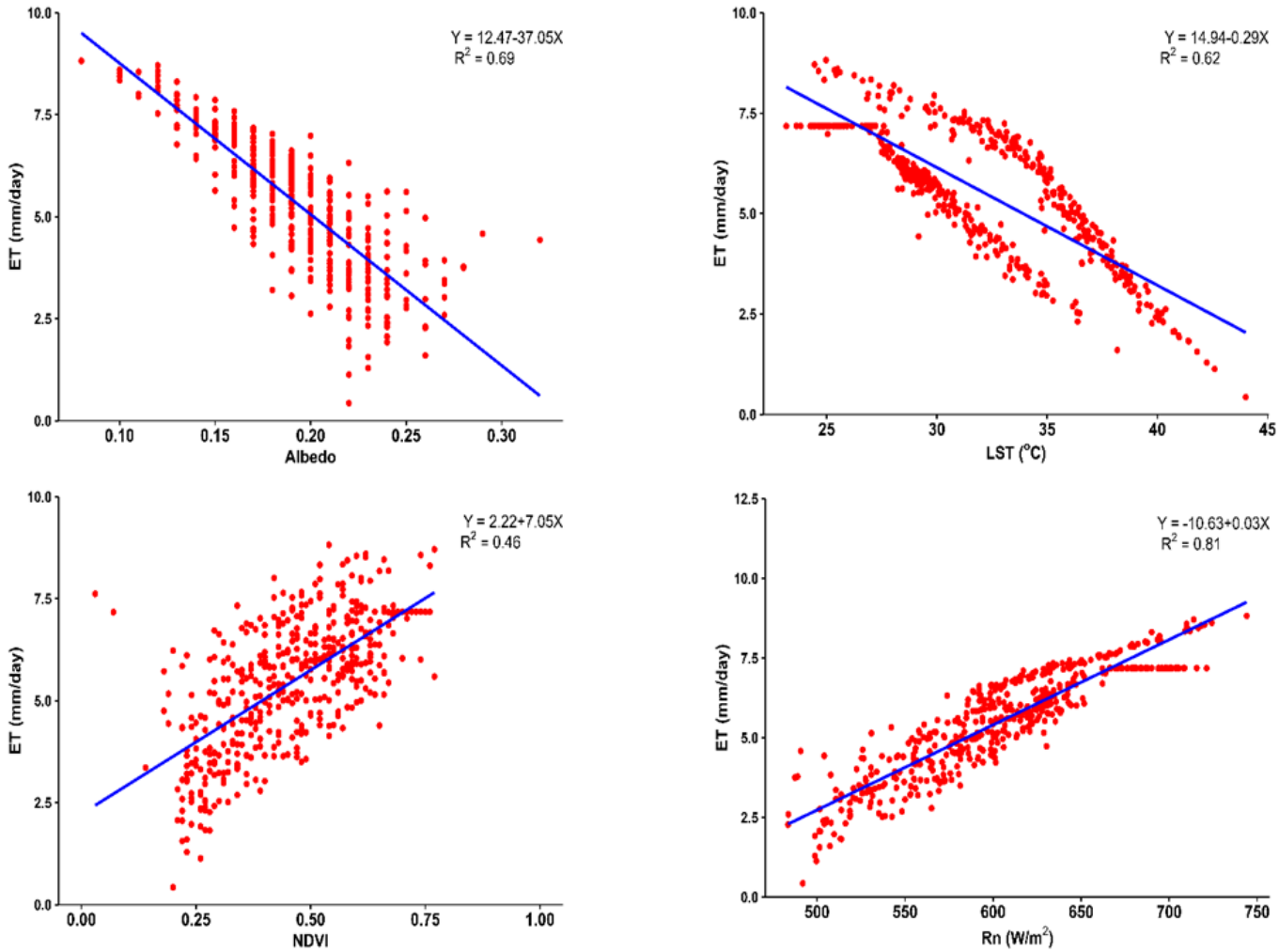

Fig. 11. Effect of surface parameters on daily evapotranspiration

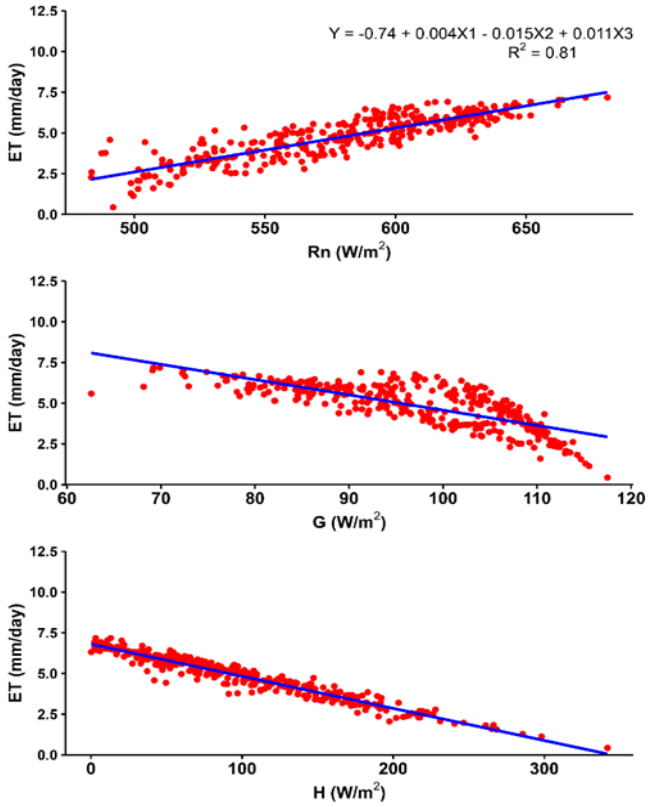

Fig. 13. Influence of various surface energy balance components on actual evapotranspiration

evapotranspiration (6.64 mm/day). The southern part of the lower Bhavani basin has a thin and sparse vegetation cover comprised of drylands, resulting in higher albedo and lower NDVI over other parts of cropland and lower evapotranspiration rates. Crops cultivated in the study area are primarily irrigated and irrigation ensures the availability of soil moisture for the evapotranspiration process. The research findings revealed that surface parameters significantly impact the spatial and temporal distribution of evapotranspiration (Fig. 11).

Similarly, surface energy balance components such as net radiation, soil heat and sensible heat fluxes were related to daily evapotranspiration (Fig. 12 and 13). It was found that daily actual evapotranspiration increased with net radiation and exhibited a positive linear relationship. However, soil and sensible heat flux are inversely correlated with evapotranspiration. The results typically demonstrated that latent heat flux increased with net radiation, yielding a higher evapotranspiration rate. The relationship of sensible heat and soil heat fluxes with net radiation flux is primarily governed by vegetation cover, surface characteristics and aerodynamic conditions.

Conclusion

The daily actual evapotranspiration estimated using the SEBAL algorithm was highly comparable with pan evaporation, which confirmed that SEBAL provides reliable estimates and can be utilized to compute regional-level evapotranspiration in diversified landscapes. The study found that the algorithm works well in different land use classes, where surface characteristics and hydrothermal conditions notably influenced the spatial distribution of evapotranspiration. A higher amount of evapotranspiration was observed in flooded vegetation and water bodies among different land use classes and the sensitivity of SEBAL to variations in surface conditions was also highlighted. Further, the study demonstrated that surface parameters, particularly net radiation, significantly influenced the evapotranspiration rates and underscored the algorithm's capacity to account for environmental variability. The research findings are particularly significant for managing water resources in lower Bhavani basin regions where intensive agriculture with high water demand crops is being practised, paving the way for sustainable water management and food security.

Acknowledgements

The authors thank the Centre for Water and Geospatial Studies, Tamil Nadu Agricultural University, Coimbatore, for extending their guidance and technical assistance in conducting this research. This research received external funding from the World Bank, Tamil Nadu Irrigated Agriculture Modernization Project (Grant number IFHRMS DPC No. 2415-01-120-PF30903).

Authors' contributions

PP: Conceptualization, Data curation, Software, Formal analysis, Writing - original draft. SP: Conceptualization, Methodology, Supervision, Funding acquisition, Writing - review & editing. APS: Writing - original draft, Methodology, Validation. KPR: Methodology, Formal analysis. SS: Resources, Visualization. KV: Writing - review & editing. PK: Writing - review & editing

Compliance with ethical standards

Conflict of interest: Authors do not have any conflict of interest to declare

Ethical issues: None

References

1. Zhang K, Chen H, Ma N, Shang S, Wang Y, et al. A global dataset of terrestrial evapotranspiration and soil moisture dynamics from 1982 to 2020. Scientific Data. 2024; 11(1):445. https://doi.org/10.1038/s41597-024-03271-7
2. Xu S, Yu Z, Yang C, Ji X, Zhang K. Trends in evapotranspiration and their responses to climate change and vegetation greening over the upper reaches of the Yellow River Basin. Agricultural and Forest Meteorology. 2018; 263:118-29. https://doi.org/10.1016/j.agrformet.2018.08.010
3. Novak V. Evapotranspiration in the soil-plant-atmosphere system. In: Novak V, editor. Evapotranspiration: a component of the water cycle. Dordrecht. 2012; 1-13. https://doi.org/10.1007/978-94-007-3840-9_1
4. Katul GG, Oren R, Manzoni S, Higgins C, Parlange MB. Evapotranspiration: A process driving mass transport and energy

exchange in the soil-plant-atmosphere-climate system. Reviews of Geophysics. 2012; 50(3):1-25. https://doi.org/10.1029/2011RG000366

5. Li ZL, Tang R, Wan Z, Bi Y, et al. A review of current methodologies for regional evapotranspiration estimation from remotely sensed data. Sensors. 2009; 9(05):3801-53. https://doi.org/10.3390/s90503801
6. Fisher JB, Melton F, Middleton E, Hain C, Anderson M, et al. The future of evapotranspiration: Global requirements for ecosystem functioning, carbon and climate feedbacks, agricultural management and water resources. Water Resources Research. 2017; 53(4):2618-26. https://doi.org/10.1002/2016WR020175
7. Chandel A. Satellite-Based Remote Sensing Approaches for Estimating Evapotranspiration from Agricultural Systems. In: Priyadarshan PM, Jain SM, Penna S, Al-Khayri, JM, editors. Digital Agriculture: A Solution for Sustainable Food and Nutritional Security. Switzerland: Cham; 2024. 281-23. https://doi.org/10.1007/978-3-031-43548-5_9
8. Dimitriadou S, Nikolakopoulos KG. Evapotranspiration trends and interactions in light of the anthropogenic footprint and the climate crisis: A review. Hydrology. 2021; 8(4):163. https://doi.org/10.3390/hydrology8040163
9. Raza A, Hu Y, Acharki S, Buttar NA, et al. Evapotranspiration importance in water resources management through cutting-edge approaches of remote sensing and machine learning algorithms. In: Pande CB, Kumar M, Kushwaha NL, editors. Surface and groundwater resources development and management in semi-arid region: strategies and solutions for sustainable water management. Switzerland: Cham; 2023. 1-20. https://doi.org/10.1007/978-3-031-29394-81
10. Acharya B, Sharma V. Comparison of satellite driven surface energy balance models in estimating crop evapotranspiration in semi-arid to arid inter-mountain region. Remote Sensing. 2021; 13 (9):1822. https://doi.org/10.3390/rs13091822
11. Zhang K, Kimball JS, Running SW. A review of remote sensing based actual evapotranspiration estimation. Wiley interdisciplinary reviews: Water. 2016; 3(6):834-53. https://doi.org/10.1002/wat2.1168
12. Ghorbanpour AK, Kisekka I, Afshar A, Hessels T, et al. Crop water productivity mapping and benchmarking using remote sensing and Google Earth Engine cloud computing. Remote Sensing. 2022; 14(19):4934. https://doi.org/10.3390/rs14194934
13. A Pawar PS, Misra AK, Rawat KS. Estimation and validation of actual evapotranspiration for wheat crop using SEBAL model over Hisar district, Haryana, India. Current Science. 2017; 10:134-41. https://doi.org/10.18520/cs/v113/i01/134-141
14. Bastiaanssen WG, Menenti M, Feddes RA, Holtslag AA. A remote sensing surface energy balance algorithm for land (SEBAL). 1. Formulation. Journal of Hydrology. 1998; 212:198-212. https://doi.org/10.1016/S0022-1694(98)00253-4
15. Cha M, Li M, Wang X. Estimation of seasonal evapotranspiration for crops in arid regions using multisource remote sensing images. Remote Sensing. 2020; 12(15):2398. https://doi.org/10.3390/rs12152398
16. Liou YA, Kar SK. Evapotranspiration estimation with remote sensing and various surface energy balance algorithms - A review. Energies. 2014; 7(5):2821-49. https://doi.org/10.3390/en7052821
17. Tan L, Zheng K, Zhao Q, Wu Y. Evapotranspiration estimation using remote sensing technology based on a SEBAL model in the upper reaches of the Huaihe river basin. Atmosphere. 2021; 12 (12):1599. https://doi.org/10.3390/atmos12121599
18. Shamloo N, Taghi Sattari M, Apaydin H, Valizadeh Kamran K, Prasad R. Evapotranspiration estimation using SEBAL algorithm integrated with remote sensing and experimental methods. International Journal of Digital Earth. 2021; 14(11):1638-58. https://doi.org/10.1080/17538947.2021.1962996
19. Ghaderi A, Dasineh M, Shokri M, Abraham J. Estimation of actual evapotranspiration using the remote sensing method and SEBAL algorithm: a case study in Ein Khosh Plain, Iran. Hydrology. 2020; 7(2):36. https://doi.org/10.3390/hydrology7020036
20. Bastiaanssen WG. SEBAL-based sensible and latent heat fluxes in the irrigated Gediz Basin, Turkey. Journal of Hydrology. 2000; 229 (1-2):87-100.
21. Bastiaanssen WG, Noordman EJ, Pelgrum H, Davids G, Thoreson BP, Allen RG. SEBAL model with remotely sensed data to improve water-resources management under actual field conditions. Journal of Irrigation and Drainage Engineering. 2005; 131(1): 85-93. https://doi.org/10.1061/(ASCE)0733-9437(2005)131:1(85)
22. Bastiaanssen WG, Pelgrum H, Wang J, Ma Y, Moreno JF, et al. A remote sensing surface energy balance algorithm for land (SEBAL). : Part 2: Validation. Journal of Hydrology. 1998; 212:213-29. https://doi.org/10.1016/S0022-1694(98)00254-6
23. Kong J, Hu Y, Yang L, Shan Z, Wang Y. Estimation of evapotranspiration for the blown-sand region in the Ordos basin based on the SEBAL model. International Journal of Remote Sensing. 2019; 40(5-6):1945-65. https://doi.org/10.1080/01431161.2018.1508919
24. Chen X, Yu S, Zhang H, Li F, Liang C, Wang Z. Estimating the actual evapotranspiration using remote sensing and SEBAL model in an arid environment of Northwest China. Water. 2023; 15(8):1555. https://doi.org/10.3390/w15081555
25. Abrishamkar M, Ahmadi A. Evapotranspiration estimation using remote sensing technology based on SEBAL algorithm. Iranian Journal of Science and Technology, Transactions of Civil Engineering. 2017; 41:65-76. https://doi.org/10.1007/s40996-016-0036-x
26. Sun Z, Wei B, Su W, Shen W, et al. Evapotranspiration estimation based on the SEBAL model in the Nansi Lake Wetland of China. Mathematical and Computer Modelling. 2011; 54(3-4):1086-92. https://doi.org/10.1016/j.mcm.2010.11.039
27. Yang L, Li J, Sun Z, Liu J, et al. Daily actual evapotranspiration estimation of different land use types based on SEBAL model in the agro-pastoral ecotone of northwest China. Plos One. 2022; 17 (3). https://doi.org/10.1371/journal.pone.0265138
28. Sugathan N, Biju V, Renuka G. Influence of soil moisture content on surface albedo and soil thermal parameters at a tropical station. Journal of Earth System Science. 2014; 123:1115-28. https://doi.org/10.1007/s12040-014-0452-x
29. Zhang X, Jiao Z, Zhao C, Qu Y, Liu Q, et al. Review of land surface albedo: variance characteristics, climate effect and management strategy. Remote Sensing. 2022; 14(6). https://doi.org/10.3390/rs14061382
30. Singh S, Kushwaha SK, Jain K. A Correlation analysis of land surface temperature and evapotranspiration in AN urban setting. The International Archives of the Photogrammetry, Remote